ECCOMAS Thematic Conference

Multibody Dynamics 2025

12th ECCOMAS Thematic Conference on Multibody Dynamics

BOOK OF ABSTRACTS

Program included

13 - 18 July 2025
University of Innsbruck | Innsbruck | Austria

edited by
Johannes Gerstmayr - Peter Manzl - Michael Pieber - Andreas Zwölfer

universität innsbruck

Title: Book of Abstracts
12th ECCOMAS Thematic Conference on Multibody Dynamics

Edited by:

Johannes Gerstmayr, University of Innsbruck, Austria
Peter Manzl, University of Innsbruck, Austria
Michael Pieber, University of Innsbruck, Austria
Andreas Zwölfer, Technical University of Munich, Germany

Graphic Design:
Peter Manzl

ISBN:
978-3-200-10587-4

First edition, July 2025

Kinematic Analysis of a Parallel-actuated Cylindrical Joint

Paula Mollá-Santamaría[1], Adrián Peidró[1,*], Marc Fabregat-Jaén[1], Luis Payá[1], Óscar Reinoso[1,2]

[1]Instituto de Investigación en Ingeniería
Miguel Hernández University
Avda Universidad s/n, 03202 Elche, Spain
*Corresponding author: apeidro@umh.es

[2]Fundación ValgrAI,
Camí de Vera s/n, Edificio 3Q, 46022
Valencia, Spain

EXTENDED ABSTRACT

1 Introduction

Cylindrical joints are often used as passive joints in parallel robots, but also actuated, as in the 3CRS [1] 3CPU [2], 3CCR [3], 6RRCRR [4], 3CPPRR [5], or 2CRRH [6] robots, where C, R, S, P, U, and H stand for cylindrical, rotational, spherical, prismatic, universal, and helical joints (underlining means actuated). Actuating cylindrical joints is not simple. One option is to build the actuated C-joint as a pair of conventional linear and rotational actuators in series, as in [1]. Another option is to use a ball-screw spline mechanism like [5]. Finally, a third innovative way is to implement the actuated C-joint through a differential RHHR closed kinematic chain, as in [6]. Due to their arrangements of actuators, these options for actuating C-joints are unpractical for the quadruped robot of Figure 1a, whose purpose is to walk and bend to climb trees, which requires articulating its front and rear segments through an actuated cylindrical joint. For this reason, we will explore the possibility of using two linear actuators in parallel to drive the cylindrical joint that articulates these segments, as sketched in Figure 1a, which is a simpler and stiffer implementation. This arrangement results in the 2UPS-C parallel mechanism, whose kinematics will be studied in this abstract.

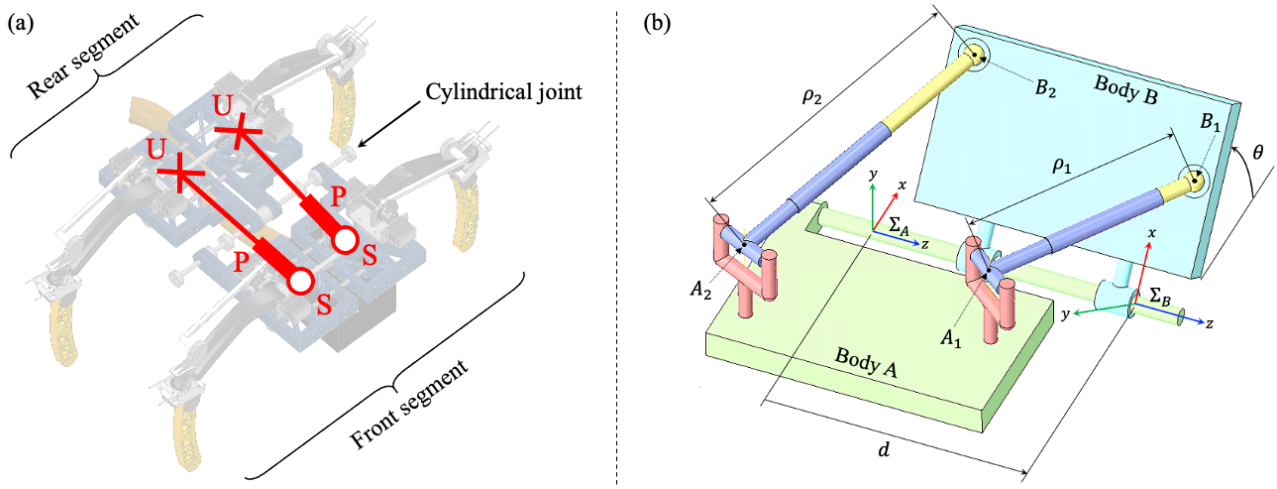

Figure 1: (a) Quadruped robot presented in [7]. (b) 2UPS-C parallel mechanism.

2 Kinematic analysis

The 2UPS-C mechanism of Figure 1b has two bodies A,B connected by a passive C-joint and two UPS limbs. A reference frame Σ_A attached to A has its z axis along the C-joint, and another frame Σ_B attached to B is obtained by translating Σ_A along z by d and rotating it about z by θ, where (θ, d) are the degrees of freedom of the C-joint. Constant coordinates of the centers A_i (respectively B_i) of the universal (resp. spherical) joints expressed in frame Σ_A (resp. Σ_B) are stored in the 3x1 column vectors $\mathbf{a}_i$ (resp. $\mathbf{b}_i$), for $i = 1, 2$. Distances between A_i and B_i are denoted by ρ_i and controlled by linear actuators. From Figure 1b:

$$\left\| [0,0,d]^T + \mathbf{R}_z(\theta)\mathbf{b}_1 - \mathbf{a}_1 \right\|^2 = \rho_1^2 \quad , \quad \left\| [0,0,d]^T + \mathbf{R}_z(\theta)\mathbf{b}_2 - \mathbf{a}_2 \right\|^2 = \rho_2^2 \tag{1}$$

where $\mathbf{R}_z(\theta)$ is a 3x3 rotation matrix of angle θ about axis z. The forward kinematic problem (FKP) consists in solving (θ, d) from (1) when ρ_i are known. To solve this analytically, note that the left-hand sides of (1) are quadratic in d and linear in $\sin\theta$ and $\cos\theta$, from which one can easily solve the sine and cosine of θ in terms of d, obtaining $\sin\theta = f(d)$ and $\cos\theta = g(d)$. Then, angle θ is eliminated by imposing $\sin^2\theta + \cos^2\theta = 1$, which yields a final equation $f^2(d) + g^2(d) = 1$ that is quartic in d. Thus, the FKP has up to four real solutions, termed *assembly modes*. Different assembly modes converge at input singularities, which are configurations at which the Jacobian matrix of the left-hand sides of (1) with respect to (θ, d) becomes singular.

3 Example

The CAD design shown in Figure 1b has the following placements of joints (units will be meters and radians): $\mathbf{a}_1 = [-0.1, 0.0875, 0.15]^T$, $\mathbf{a}_2 = [-0.15, 0.0875, -0.05]^T$, $\mathbf{b}_1 = [0.116, 0.0225, 0.034]^T$ and $\mathbf{b}_2 = [0.168, 0.0225, -0.178]^T$, with actuator lengths $\rho_1 = 0.193$ and $\rho_2 = 0.261$ represented by point P in Figure 2a. Solving the FKP yields four solutions, two of them real: $(\theta = 0.9485, d = 0.2363)$, $(\theta = 1.1657, d = -0.0281)$, $(\theta = -1.8477 \pm 0.0942i, d = 0.1056 \pm 0.115i)$, where the first one is represented in Figure 1b. Figure 2a represents the (ρ_1, ρ_2) plane, where blue curves represent input singularities. Another point Q is represented in Figure 2a for which solutions to the FKP are all real: $S_1(\theta = 1.609, d = 0.3)$, $S_2(\theta = 3.8, d = 0.2)$, $S_3(\theta = 2, d = -0.08)$, and $S_4(\theta = 3.6, d = -0.0073)$. These are represented in Figure 2b, which also shows the input singularities in the (θ, d) plane. Singularity curves in Figure 2a exhibit a cusp point, which are well-known to enable transitions between some FKP solutions without meeting singularities. For example, starting at solution S_3 and encircling the cusp counter-clockwise as with the red trajectory in Figure 2a transforms this solution into S_2, as demonstrated in Figure 2b.

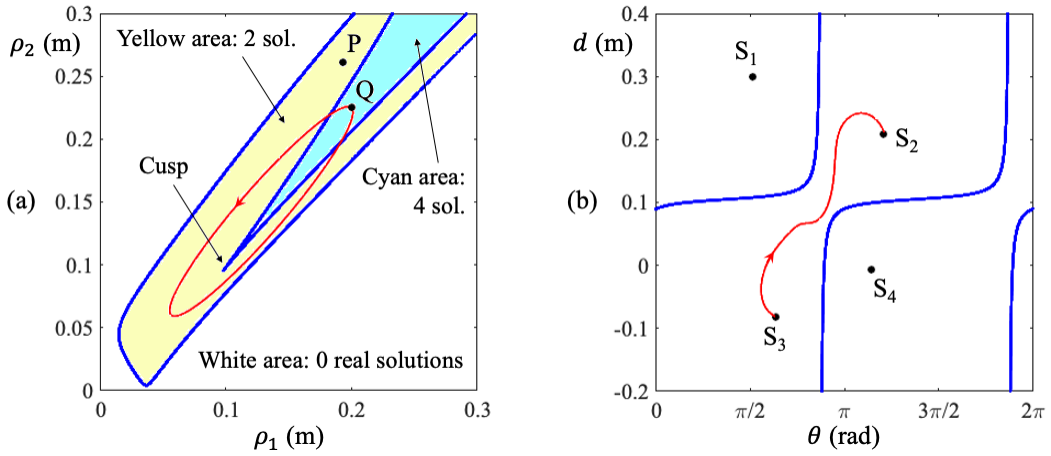

Figure 2: (a) Space (ρ_1, ρ_2) of actuated joints of the 2UPS-C parallel mechanism. (b) Space (θ, d) of the cylindrical joint.

4 Conclusions and future work

The 2UPS-C parallel mechanism admits analytical solution to its FKP and is cuspidal. In the future, we will address its optimal kinematic and dynamic design to serve as the central joint of the quadruped robot shown in Figure 1a, considering that, in the actual robot, additional prismatic joints change the distance between universal (respectively spherical) joints in body A (resp. B).

Acknowledgments

This work is part of the project PID2023-149575OB-I00, funded by MICIU/AEI/10.13039/501100011033 and by FEDER, UE.

References

[1] A. V. Nguyen, B. C. Bouzgarrou, K. Charlet and A. Béakou. Static and dynamic characterization of the 6-Dofs parallel robot 3CRS. Mechanism and Machine Theory, 93:65-82, 2015.

[2] L. Carbonari, M. Callegari, G. Palmieri and M-C. Palpacelli. A new class of reconfigurable parallel kinematic machines. Mechanism and Machine Theory, 79:173-183, 2014.

[3] Y. Zhang, Y. Zhao, X. Jing, and X. Li. Type synthesis of uncoupled translational parallel manipulators based on actuation wrench screw theory. Advances in Mechanical Engineering, 10(1):1–10, 2018.

[4] Y. Zhang, H. Han, H. Zhang, Z. Xu, Y. Xiong, K. Han and Y. Li. Acceleration analysis of 6-RR-RP-RR parallel manipulator with offset hinges by means of a hybrid method. Mechanism and Machine Theory, 169:104661, 2022.

[5] Y. Jin, I-M. Chen and G. Yang. Structure synthesis and singularity analysis of a parallel manipulator based on selective actuation. In Proceedings of the 2004 IEEE Intl. Conf. on Robotics and Automation, pages 4533–4538, 2004.

[6] T. Harada, T. Friedlaender, and J. Angeles. The development of an innovative two-DOF cylindrical drive: Design, analysis and preliminary tests. In Proceedings of the 2014 IEEE Intl. Conf. on Robotics and Automation, pages 6338–6344, 2014.

[7] P. Mollá-Santamaría, A. Peidró, M. Fabregat-Jaén, L. M. Jiménez and Ó. Reinoso. Motion analysis of a tree-climbing robot. In Book of Abstracts of the Mechanism and Machine Theory Symposium, pages 381–382, 2024.